

Persistent skewness of a strongly active scalar

Jie Zhang* and X. L. Wu

Department of Physics and Astronomy, University of Pittsburgh, Pittsburgh, Pennsylvania 15260, USA

(Received 17 January 2009; published 8 April 2009)

We present a skewness measurement of the density fluctuations $\delta\bar{\rho}_l$ on scales l in a vertical turbulent soap film driven by a temperature gradient. Unlike the temperature difference δT_l in Rayleigh-Bénard convection, the density difference in the film is strongly active because $\delta\bar{\rho}_l/\bar{\rho} \gg \delta T_l/\bar{T}$, where the over-bar indicates the mean. Our results show persistent nonzero skewness $S_y(l) \equiv \langle \delta\bar{\rho}_l^3 \rangle / \langle \delta\bar{\rho}_l^2 \rangle^{3/2}$ on different scales along the gravity direction \hat{y} ; $S_y(l)$ is positive for small l and negative for large l . The sign switch occurs approximately at the Bolgiano length scale l_B . The simultaneous presence of positive and negative skewnesses is interpreted here as a result of the structures of rising and falling plumes in a strongly stratified medium.

DOI: 10.1103/PhysRevE.79.045301

PACS number(s): 47.27.te, 47.55.Hd, 47.55.pb

In turbulence, the third-order structure function of the longitudinal velocity difference, $\langle \delta v_\ell^3 \rangle \equiv \langle \{ [\vec{v}(\vec{x} + \vec{\ell}) - \vec{v}(\vec{x})] \cdot \vec{\ell} / \ell \}^3 \rangle$, is a measure of the kinetic energy flux on the scale of ℓ in an inertial range [1,2]. The existence of an inertial range implies that this third-order structure function cannot be zero and can even change sign in nonisotropic turbulence, depending on the location of measurement [3]. In contrast, such a correspondence does not exist for a scalar quantity, and the third-order structure function of the scalar is expected to vanish in homogeneous and isotropic turbulence [4]. However, both numerical simulations and laboratory experiments found nonzero skewness of passive scalars in Navier-Stokes turbulence when a linear scalar gradient was imposed on the system scale [5–7]. These results are surprising and appear to contradict the well-known property of turbulence; i.e., scalar distributions on small scales are expected to be well mixed (homogeneous and isotropic) due to a series of cascade steps. Recent experiments also showed that the same persistence effect occurred in an active scalar, the temperature in Rayleigh-Bénard convection (RBC) in water (Prandtl number $\text{Pr} \approx 7$) [8–10] and in mercury ($\text{Pr} \approx 0.024$) [11]. The skewness calculated using temperature time series in water was found to exist for time scales τ shorter than the Bolgiano time τ_B ($\tau < \tau_B$). However, for $\tau > \tau_B$, no skewness was observed [8–10]. For low-Prandtl-number systems [11], the peculiar properties of the skewness near a thermal boundary layer led the investigators to conclude that turbulence in such a system may not be driven by thermal plumes.

In this paper we present experimental results concerning the skewness of a strongly active scalar, i.e., the two-dimensional (2D) density ($\rho_2 \equiv \rho_0 h$) of a vertical soap film subject to a large in-plane temperature gradient, where ρ_0 is the density of water and h is the local film thickness. Due to gravity, the film is strongly stratified [12,13], creating a mean thickness gradient vertically along the film [see Fig. 2(b)]. Contrary to our intuition that a stable density gradient suppresses fluid motion, we found in our experiment that this mean density gradient is the source of inhomogeneity, creating intense 2D density fluctuations $\delta\rho_2$ that amount to $\sim 30\%$

of the mean $\bar{\rho}_2$ [12]. This magnitude of fluctuations is considerably greater (~ 30 times) than those typically encountered in RBC and therefore provides a useful test ground for statistical descriptions of an active scalar in turbulence. For conciseness of the notation, in what follows the subscript 2 will be dropped. We found that the skewness $S_y(l) \equiv \langle \delta\bar{\rho}_l^3 \rangle / \langle \delta\bar{\rho}_l^2 \rangle^{3/2}$ along the gravitational direction \hat{y} in the film is of the order of unity in both large [$S_y(l) \propto -1$, $l \gg l_B$] and small [$S_y(l) \propto +1$, $l \ll l_B$] scales, and approaches zero approximately at the Bolgiano scale l_B . This result can be qualitatively explained by the structures of rising and falling plumes, and the large skewness can be shown to be consistent with Bolgiano's theory of turbulence in a stably stratified fluid [14,15].

In this experiment, an infrared camera (Jade LWIR, 320 \times 256 pixels) was used to measure the 2D mass density variations $\bar{\rho}(x, y) = \rho_0 \delta h(x, y)$ in the film, where $\delta h(x, y) = h(x, y) - \bar{h}(x, y)$ is the local variation in the film thickness and $\bar{h}(x, y)$ is the mean. The camera has a spectral range of $8 < \lambda < 13 \mu\text{m}$, and the imaging geometry allows the thermal radiation $I(x, y)$ of different fluid elements in the film to be mapped onto the camera's ir sensor array. The camera operates at a shutter speed of 1 ms in order to resolve the fastest motion of the flow, ~ 2 ms, which is estimated from the spatial resolution of the camera and ν_{rms} of the flow. In our previous work using a single ir detector, it was shown that the ir intensity $I(x, y)$ is proportional to temperature as $I \propto sT^4$, and the variation of the intensity $\delta I(x, y)$ gives an accurate determination of the film thickness variations $\delta h(x, y)$ due to the strong h dependence in the thermal emissivity $s(h)$ of the film [12,16]. The full-field ir imaging technique used in this work allows the density difference $\delta\bar{\rho}_l$ on scales l to be directly measured without invoking the Taylor frozen-turbulence assumption. Most significantly, the technique eliminates the ambiguity of the direction of the scalar skewness when measured using a single detector in a system with no mean flow [8,11].

The soap film convection setup has been previously described [12]. Here only information relevant to the present experiment is provided. Thermal images are taken from a vertically suspended ($2 \times 2 \text{ cm}^2$) soap film that is subject to a temperature difference $\Delta T = 67 \text{ K}$ along the gravity direction, cold at the top and hot at the bottom. The Rayleigh number

*Present address: Department of Physics, Duke University, Box 90305, Durham, NC 27708, USA.

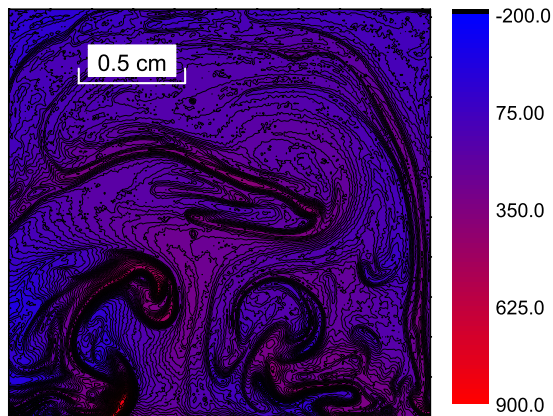


FIG. 1. (Color online) Snapshot of the 2D density field $\tilde{\rho}(x,y) = \rho_0(h(x,y) - \bar{h}(x,y))$. Images are acquired at 30 frames/s by the ir camera. The labels of the color codes are in arbitrary units.

of the system is $Ra(\equiv \alpha \Delta T g H^3 / \nu \kappa) \approx 8.4 \times 10^6$, where g is the gravitational constant, H (≈ 2 cm) is the film height, and α , ν , and κ are respectively the thermal expansion coefficient, the kinematic viscosity, and the thermal diffusivity of water. Here, ν is mainly determined by the water, and decreases from 0.012 cm^2/s at 12 $^\circ\text{C}$ to 0.004 cm^2/s at 70 $^\circ\text{C}$; κ is less sensitive to temperature, changing by only a few percent in the same temperature interval. In a strong-convection regime, which is the case in this experiment, most of the temperature drop is within (~ 1 mm) the thermal boundary layer. Hence, the temperature variation in the bulk of the film is expected to be considerably less than ΔT , and ν may be treated as constant. The typical velocity in the film measured by particle imaging velocimetry is $v_{\text{rms}} \approx 5.5$ cm/s , corresponding to a Reynolds number $Re(\equiv v_{\text{rms}} H / \nu) \approx 10^3$.

Figure 1 is a typical 2D density difference image $\tilde{\rho}(x,y) \equiv \rho_0 \delta h(x,y)$ acquired by the ir camera. Thermal plumes of various sizes are clearly seen. One observes that the rising plumes have a well-defined mushroom shape, consisting of a cap and a stem. In contrast, the shape of a falling plume is less well defined. When a plume rises and then falls, its size increases with time. Since the convection takes place in a closed cell, there are considerable interactions between plumes generated at different times and locations, resulting in highly contorted patterns as seen in the figure. To quantify our observations, the density-density correlation function $C(\vec{l}) = \langle \tilde{\rho}(\vec{r} + \vec{l}) \tilde{\rho}(\vec{r}) \rangle / \langle \tilde{\rho}(\vec{r})^2 \rangle$ was calculated and is displayed in Fig. 2 for \vec{l} along the \hat{x} (\circ) and the \hat{y} (\square) axis, where the angular brackets denote both the spatial and the time average. The correlation function shows two different regimes. For small $|\vec{l}|$, the fluctuations are nearly “isotropic” as indicated by the nearly identical decay length of $C(l)$ in both the \hat{x} and the \hat{y} directions. Using the exponential function $C(\vec{l}) = \exp(-|\vec{l}|/\xi)$ to mimic this short-distance behavior, we found the correlation length $\xi \approx 0.22 \pm 0.05$ cm for both directions. For large $|\vec{l}|$, the density fluctuations are highly anisotropic; they are more strongly correlated along the horizontal direction than perpendicular to it. This is consistent with the fact

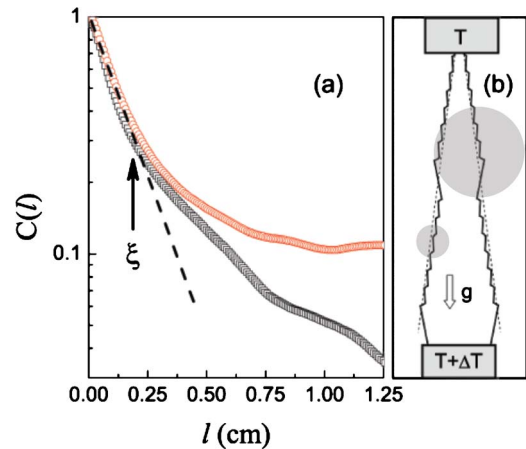


FIG. 2. (Color online) (a) Density-density correlation functions measured along the horizontal \hat{x} (\circ) and the vertical \hat{y} (\square) axes. (b) Sketch of the structures of 2D density profiles (not to scale). The dotted line denotes the mean density profile. The indentations depict plume structures (see text for details). The small (large) circle indicates a small (large) ramp-cliff structure, resulting from a rising (falling) plume.

that a stable density gradient organizes flow into layered structures perpendicular to gravity [17]. We note that the density fluctuation being isotropic on small scales but anisotropic on large scales is one of the key assumptions of Bolgiano’s theory, and our measurement shows that such a division of length scales is indeed reasonable. Quantitatively, the measured short-distance correlation length ξ is in good agreement with the Bolgiano scale l_B (≈ 0.26 cm) determined from a velocity measurement [18], lending further support to this assumption.

A long-standing issue of scalar turbulence is the persistence of local anisotropy of the scalar [6]. This issue can be studied in our system by direct measurements of the skewness $S_y(l) \equiv \langle \tilde{\rho}_l^3 \rangle / \langle \tilde{\rho}_l^2 \rangle^{3/2}$ along the vertical direction for various scales l , where $\tilde{\rho}_l \equiv \tilde{\rho}(\vec{r} + l\hat{y}) - \tilde{\rho}(\vec{r})$. Figure 3 displays the probability density function of $\tilde{\rho}_l$ for l spanning nearly two decades in length ($80 \mu\text{m} \leq l \leq 0.7$ cm). A conspicuous feature of $P(\tilde{\rho}_l)$ is the asymmetry; it is skewed toward positive

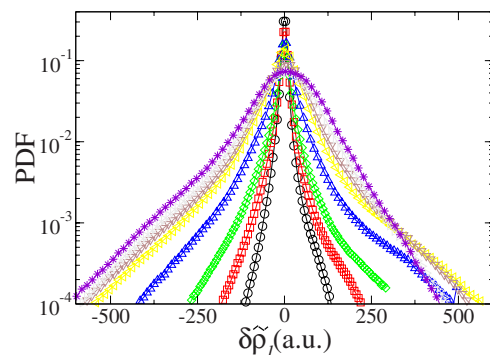


FIG. 3. (Color online) Probability density functions of 2D density difference $\tilde{\rho}_l \equiv \tilde{\rho}(x,y+l) - \tilde{\rho}(x,y)$, where positive y is along the gravity \vec{g} direction. Different symbols correspond to $l=0.008$ (\circ), 0.016 (\square), 0.031 (\diamond), 0.062 (\triangle), 0.125 (\triangleleft), 0.25 (∇), 0.5 (\triangleright), and 0.7 ($*$) cm.

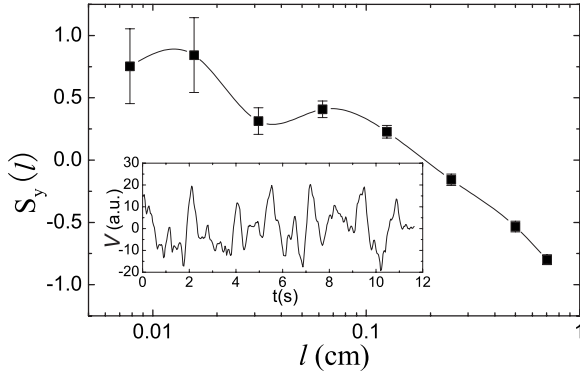


FIG. 4. Skewness $S(l) (\equiv \langle \tilde{\rho}_l^3 \rangle / \langle \tilde{\rho}_l^2 \rangle^{3/2})$ along the vertical direction as a function of l . The inset is the total potential energy (V), as a function of time, t . Coherent oscillations on the time scale of ~ 1 s are observed.

$\tilde{\rho}_l$ for small l and toward negative $\tilde{\rho}_l$ for large l . The changing sign of $S_y(l)$ precludes self-similarity of the density fluctuations on all scales. Quantitative measurements of $S_y(l)$ for various l are presented in Fig. 4. Here we observed that for the smallest ($l_{\min} = 80 \mu\text{m}$) and the largest scales ($l_{\max} = 0.7$ cm), $|S_y(l)|$ is of the order of unity and decreases monotonically as l increases. We also noticed that the location where $S_y(l)$ becomes zero is very close to the measured $\xi \approx 0.22$ cm, indicating that $S_y(l)$, similarly to $C(\bar{r})$, can be a useful diagnosis of different flow regimes. To our knowledge, this is the first reported case of the simultaneous presence of positive and negative skewness on different length scales in a given system. As will be discussed below, there are reasons to believe that this is a general feature of convective turbulence in stably stratified fluids, which are common in nature. We would also like to point out that, because $S_y(l) \approx 1$ for $l \ll l_B$, the scalar turbulence cannot be strictly isotropic on small scales in spite of the fact that $C(\bar{r})$ decays similarly along the \hat{x} and the \hat{y} directions. In other words, $S_y(l)$ and $C(\bar{r})$ probe different aspects of isotropy of the system.

To appreciate the problem at hand for an active scalar, it is helpful first to examine behaviors of passive-scalar turbulence. The persistence of anisotropy is a peculiar feature of this type of turbulence, and, as pointed out by early investigators, it contradicts the fundamental assumption of Kolmogorov theory, which postulates that turbulent fluctuations on small scales are isotropic [5,7]. The expectation of isotropic scalar fluctuations $\theta(\vec{x})$ on small scales follows from the Obukhov-Corsin theory, which shows that the second-order structure function $F_2(l) \equiv \langle [\theta(l) - \theta(0)]^2 \rangle$ in the inertial range scales in the same way as the second-order velocity structure function, i.e., $F_2(l) \sim l^{2/3}$. In typical experiments, the scalar fluctuations in the inertial range are supplied continuously from large-scale inhomogeneity, which can be mimicked by a gradient Θ' . If this gradient is maintained in the presence of turbulence, it is expected that $F_3(l)/l \propto \Theta' F_2(l)$. It follows that $S(l) = F_3(l)/F_2(l)^{3/2} \sim (l/l_0)^{2/3}$, where l_0 is an outer scale of turbulence. This relation suggests that the skewness should decrease with l for fixed Re or vanish as $\text{Re}^{-1/2}$ as Re is increased. However, this small-scale isotropization effect has not been convincingly observed in laboratory measurements [6] or in numerical simulations [5].

In what follows, we wish to show that for an active scalar, such as the 2D density of our soap film which couples strongly to gravity, the persistence of skewness is to be expected on both large and small scales. It follows from Bolgiano's theory, which assumes $\chi \equiv \langle \partial \rho^2 / \partial t \rangle = \langle \rho u_y \partial \rho / \partial y \rangle$ instead of $\langle \partial \rho / \partial y \rangle$ to be a constant of motion, where u_y is the vertical component of the velocity. To illustrate the point, we resort to Lumley's calculation, which generalizes Kolmogorov's 1941 theory to situations where turbulent flow interacts with another (conservative or nonconservative) field [4]. In the special case of buoyancy-driven flows, as in the present case, the energy flux in the wave number k space is given by

$$\partial \varepsilon_k / \partial k = - (g/\rho) \overline{[\delta \rho u_y]}_k, \quad (1)$$

where the subscript $[\]_k$ denotes that the quantity is expressed in terms of wave number k , and ρ is the density of the fluid. Based on a similarity assumption, the mass flux passing through a spherical shell of radius k is given by $\overline{[\delta \rho u_y]}_k = \chi^{1/2} \varepsilon_k^{1/6} k^{-5/3} \varphi((g/\rho) \chi^{1/2} \varepsilon_k^{-5/6} k^{-2/3})$. Nondimensionalizing the flux equation by introducing the variables $x = (k/k_B)^{-2/3}$ and $y = (\varepsilon_k/\varepsilon_B)^{5/6}$, Eq. (1) is reduced to

$$dy/dx = \phi(x/y), \quad (2)$$

where k_B is the Bolgiano wave number and ε_B is the energy transfer rate at that scale. The above equation can be solved in the limit $x \rightarrow 0$ (or $k \gg k_B$) and $x \rightarrow \infty$ (or $k \ll k_B$), with the result

$$\varepsilon_k = \begin{cases} \varepsilon_B [1 + (k_B/k)^{4/3}]^{2/3} \approx \varepsilon_B, & k \gg k_B, \\ (g/\rho)^{6/5} \chi^{3/5} k^{-4/5}, & k \ll k_B. \end{cases} \quad (3)$$

This derivation shows that, unlike Navier-Stokes turbulence, the exchange of turbulent kinetic energy (KE) with the gravitational potential energy (PE) is significant on large scales, giving rise to a "leaky" energy flux at small k . Consequently, the energy spectrum $E(k) \sim \varepsilon_k^{2/3} k^{-5/3} \sim k^{-11/5}$ is steeper than in the corresponding constant-density case with $E(k) \sim k^{-5/3}$. However, for k greater than k_B , the energy flux is constant, $\varepsilon_k = \varepsilon_B$, independent of k , and $E(k)$ resumes the classical Kolmogorov result, $E(k) \sim \varepsilon_B^{2/3} k^{-5/3}$. The above energy flux equations also imply that the velocity variance $\langle \delta v_l^2 \rangle$, the scalar variance $\langle \delta \rho_l^2 \rangle$, and the mass flux $\langle \delta \rho_l \delta u_{y,l} \rangle$ have the following scaling forms: $\langle \delta v_l^2 \rangle \sim l^{2/3}$, $\langle \delta \rho_l^2 \rangle \sim l^{2/3}$, $\langle \delta \rho_l \delta u_{y,l} \rangle \sim l^{2/3}$ for $l < 1/k_B$ and $\langle \delta v_l^2 \rangle \sim l^{6/5}$, $\langle \delta \rho_l^2 \rangle \sim l^{2/5}$, $\langle \delta \rho_l \delta u_{y,l} \rangle \sim l^{4/5}$ for $l > 1/k_B$. These results are consistent with Bolgiano's original derivation [14] and are also consistent with L'vov's derivation using an entropy-cascade idea [15]. For a reasonable distribution of the random variable $\delta \rho_l \delta u_{y,l}$, one expects that $\langle (\delta \rho_l \delta u_{y,l})^3 \rangle \propto \langle \delta \rho_l \delta u_{y,l} \rangle^3$. Consequently, the scalar skewness can be evaluated as $S_y(l) = \langle (\delta \rho_l \delta u_{y,l})^3 \rangle / \langle \delta \rho_l^2 \rangle^{3/2} \langle \delta u_{y,l}^2 \rangle^{3/2} \propto \langle \delta \rho_l \delta u_{y,l} \rangle^3 / \langle \delta \rho_l^2 \rangle^{3/2} \langle \delta u_{y,l}^2 \rangle^{3/2}$. Using the scaling relations derived above, it is seen that for both large ($l \gg 1/k_B$) and small ($l \ll 1/k_B$) scales, $S_y(l)$ is independent of l ($S_y(l) \propto l^0$) and is of the order of unity. This prediction is fully consistent with the data in Fig. 4, where $S_y(l) \approx 0.75$ for small and $S_y(l) \approx -0.75$ for large scales in the measurement. Since $S_y(l)$ possesses different signs at the two extremes of l , it must vanish at a certain scale l , which turns out to be close to ξ or l_B .

The physical mechanism that gives rise to the unusual $S_y(\ell)$ seen in our experiment remains to be understood. We noticed that, in a stably stratified soap film, the emission of plumes is highly asymmetric, with frequent ejections from the bottom thermal boundary layer but rarely from the top. Though the plumes are small initially, they are fast moving and are the primary source of kinetic energy for turbulent fluctuations in the film. The rising plumes expand in size, cool, and gradually lose their KE to PE. Once the plumes reach the top of the film, they start to fall and the PE is converted back to KE. The typical lifetime of a plume, from emerging to descending, is about a second, and the conversion of PE to KE takes place on large scales. When a plume rises or falls, its front is compressed, forming the characteristic shape of a mushroom. The mushroom of a falling plume is oriented opposite to the rising ones and its size is considerably larger. The compression of fluid at the leading edge of the mushroom causes a large density gradient while the trailing edge has a gentler gradient. This forms the so-called ramp-cliff (RC) structures, sketched schematically in Fig. 2(b), and is the major contribution to the skewness seen in the experiment. In the figure, the mean density (or thickness) profile is indicated by two dashed lines; the large RCs correspond to falling plumes, and the finer RCs correspond to rising ones. Since the RCs are oppositely oriented for large (falling plumes) and small (rising plumes) scales, $S_y(\ell)$ changes sign accordingly.

Based on these observations, it is clear that convective turbulence in a stably stratified fluid behaves differently from Navier-Stokes turbulence. Although there is transfer of energy from scale to scale, which in our case is from the small to the large scales [18], such a transfer is not accompanied by vigorous mixing of fluid elements. We noticed that, while plumes move about in the film, their influence on the surrounding fluid is long ranged, often causing wild oscillations. The presence of density waves in a stratified fluid is known and is readily observed in our soap film, particularly near the onset of convection [19]. When waves are involved in turbulence, new effects arise because waves can transport momen-

tum and energy without the exchange of fluid masses. There has been much debate about the effects of nonlinear density waves on the energy transfer in turbulence, including the unexpected k^{-3} energy spectrum observed in the earth atmosphere [20]. We believe that these waves also play subtle roles in our experiment, including the persistence of the skewness. To appreciate the contribution of the nonlinear density waves in our soap-film convection, we measured the total PE of the system $V = \iint_A \bar{\rho}(x, y) g y dx dy$ as a function of time t . Here the integration is over the entire area A of the film. As can be seen in the inset of Fig. 4, the V oscillates wildly with a time scale of ~ 1 s. This time scale matches reasonably well with the inverse of the Brunt-Vaisala frequency $f_{BS} [\equiv (1/2\pi) \sqrt{(\delta\rho/\rho)(g/H)}] \approx 1.9$ Hz, where the system parameters $\delta\rho/\rho \approx 30\%$ and $H = 2$ cm are used for the estimation. We note that, since fast (or short-wavelength) modes are integrated over, the remaining fluctuations represent coherent oscillation of the whole system, which is somewhat slower than the calculated f_{BS} .

In conclusion, we have measured the skewness of density fluctuations along the mean-density gradient of a flowing soap film using a full-field ir imaging technique. The skewness is found to be unity, but of different signs, for large and small scales. This unexpected effect can be explained by the structures of rising and falling plumes, which are the prominent structure of convective turbulence in the soap film. Examination of these structures suggests that turbulent mixing in our system is considerably different from conventional turbulence with a constant density. Though the flow appears to be spatiotemporally chaotic or turbulent, there are coherent oscillations in the fluid. Such oscillations are the signature of nonlinear gravitational density waves with frequencies close to f_{BS} . When turbulence is coupled to waves, mixing on small and large scales is not very efficient due to the leakage of KE to PE. We believe that this is the cause for the persistence of density skewness on different scales, and it is a general property of strongly stratified systems.

We would like to thank Y.-G. Jun for helpful discussions. This work is supported by NSF (Grant No. DMR-0242284).

-
- [1] A. N. Kolmogorov, Dokl. Akad. Nauk SSSR **30**, 9 (1941).
 [2] A. N. Kolmogorov, Dokl. Akad. Nauk SSSR **32**, 16 (1941).
 [3] C. Simand, F. Chilla, and J.-F. Pinton, Europhys. Lett. **49**, 336 (2000).
 [4] J. L. Lumley, Phys. Fluids **10**, 855 (1967).
 [5] M. Holzer and E. D. Siggia, Phys. Fluids **6**, 1820 (1994).
 [6] L. Mydlarski and Z. Warhaft, J. Fluid Mech. **358**, 135 (1998).
 [7] L. Mydlarski, A. Pumir, B. I. Shraiman, E. D. Siggia, and Z. Warhaft, Phys. Rev. Lett. **81**, 4373 (1998).
 [8] S.-Q. Zhou and K.-Q. Xia, Phys. Rev. Lett. **89**, 184502 (2002).
 [9] Q. Zhou and K.-Q. Xia, Phys. Rev. E **77**, 056312 (2008).
 [10] X. He and P. Tong, Phys. Rev. E **79**, 026306 (2009).
 [11] T. Segawa, A. Naert, and M. Sano, Phys. Rev. E **57**, 557 (1998).
 [12] J. Zhang, X. L. Wu, and K.-Q. Xia, Phys. Rev. Lett. **94**, 174503 (2005).
 [13] F. Seychelles, Y. Amarouchene, M. Bessafi, and H. Kellay, Phys. Rev. Lett. **100**, 144501 (2008).
 [14] R. Bolgiano, Jr., J. Geophys. Res. **64**, 2226 (1959).
 [15] V. S. L'vov, Phys. Rev. Lett. **67**, 687 (1991).
 [16] J. Zhang, X. L. Wu, and N. Rashidnia, Phys. Fluids **18**, 085110 (2006).
 [17] P. Billant and J.-M. Chomaz, Phys. Fluids **13**, 1645 (2001).
 [18] J. Zhang and X. L. Wu, Phys. Rev. Lett. **94**, 234501 (2005).
 [19] B. Martin and X. L. Wu, Phys. Rev. Lett. **80**, 1892 (1998).
 [20] E. Lindborg, J. Fluid Mech. **550**, 207 (2006).